



**HAL**  
open science

# Flank wear prediction in milling AISI 4140 based on cutting forces PCA for different cutting edge preparations

Lamice A Denguir, Aurélien Besnard, Guillaume Fromentin, Gérard Poulachon, Xiaowen Zhu

## ► To cite this version:

Lamice A Denguir, Aurélien Besnard, Guillaume Fromentin, Gérard Poulachon, Xiaowen Zhu. Flank wear prediction in milling AISI 4140 based on cutting forces PCA for different cutting edge preparations. *International Journal of Machining and Machinability of Materials*, 2016, 18 (3), pp.273-287. 10.1504/IJMMM.2016.076278 . hal-01333573

**HAL Id: hal-01333573**

**<https://hal.science/hal-01333573>**

Submitted on 18 Dec 2017

**HAL** is a multi-disciplinary open access archive for the deposit and dissemination of scientific research documents, whether they are published or not. The documents may come from teaching and research institutions in France or abroad, or from public or private research centers.

L'archive ouverte pluridisciplinaire **HAL**, est destinée au dépôt et à la diffusion de documents scientifiques de niveau recherche, publiés ou non, émanant des établissements d'enseignement et de recherche français ou étrangers, des laboratoires publics ou privés.

# Flank wear prediction in milling AISI 4140 based on cutting forces PCA for different cutting edge preparations

L.A. Denguir\*

Arts et Metiers ParisTech, LaBoMaP,  
Rue Porte de Paris, 71250 Cluny, France  
and

Ecole Nationale d'Ingenieurs de Monastir, LGM,  
avenue Ibn El Jazzar, 5019 Monastir, Tunisie  
Fax: +33-3-8559-5370

Email: Lamice.DENGUIR@ensam.eu

\*Corresponding author

A. Besnard, G. Fromentin and G. Poulachon

Arts et Metiers ParisTech, LaBoMaP,  
Rue Porte de Paris, 71250 Cluny, France

Email: Aurelien.BESNARD@ensam.eu

Email: Guillaume.FROMENTIN@ensam.eu

Email: Gerard.POULACHON@ensam.eu

X. Zhu

Arts et Metiers ParisTech, LaBoMaP,  
Rue Porte de Paris, 71250 Cluny, France  
and

Shanghai Jiao Tong University,  
Dong Chuan Lu Minhang, 200240 Shanghai, China  
Email: eversince@aliyun.com

**Abstract:** One of the criteria mastering the choice of a cutting tool is its wear resistance. For coated inserts, prior to the coating process, edge preparation method choice will impact their performance. So, a classification based on its impact on wear resistance is needed. Indeed, the flank wear of three coated cemented carbide inserts presenting differently prepared edges (untreated, dragging and magneto-abrasive machining) is explored experimentally. Those inserts are used to face mill the hardened AISI 4140 low alloy steel. Further, by means of the principal component analysis (PCA), correlations between the online measured cutting forces and flank wear behaviour are investigated. In view of this analysis, for each studied case, the statistical law predicting flank wear relying on cutting forces components is established with fair approximation. However, the experimental results have quantitatively shown that edge preparation could be in some cases not beneficial for tool wear resistance of the milling inserts considering either maximal or average flank wear.

**Keywords:** flank wear; cutting edge preparation; PCA; wear test.

**Reference** to this paper should be made as follows: Denguir, L.A., Besnard, A., Fromentin, G., Poulachon, G. and Zhu, X. (2016) 'Flank wear prediction in milling AISI 4140 based on cutting forces PCA for different cutting edge preparations', *Int. J. Machining and Machinability of Materials*, Vol. 18, No. 3, pp.273–287.

**Biographical notes:** L.A. Denguir holds a Mechanical Engineering degree from ENIM (Monastir, Tunisia in 2012) and an MSc in Materials and Engineering from Arts et Metiers ParisTech (France in 2013). She is currently a PhD candidate in Manufacturing from Arts et Metiers ParisTech (France in 2015). She is part of High Speed Machining team in LaBoMaP, Cluny, France. She develops her main research activities on characterising and modelling surface integrity induced by the machining process (mechanical aspects, microstructure and durability). Her work is published in peer-reviewed scientific journals and presented in international conferences.

A. Besnard received his PhD in Surface Engineering from the University of Franche-Comté (Besançon, France) in 2010. He is an Associate Professor at Arts et Metiers ParisTech since 2011. He develops his research activities at the LaBoMaP on protective coating for cutting tools and on the deposition process (physical vapour deposition). His main research interest is the control of the deposition process using simulation and experimental with the aim of optimising the coating development. His work is published in peer-reviewed scientific journals and presented in international conferences.

G. Fromentin received his PhD in Manufacturing from Arts & Métiers ParisTech, France in 2004. He was postdoc in EPFL, Switzerland and since 2006, he is an Associate Professor at Arts et Métiers ParisTech. He develops research activities at LaBoMaP Laboratory on high speed machining of difficult-to-cut materials and on modelling and optimisation of machining operation. He has been involved in several machining projects in cooperation with several academic and industrial partners in Europe. He obtained in 2013 ability to supervise research diploma and during 2015, he was Visiting Professor in WZL Institute at RWTH University, in Aachen, Germany.

G. Poulachon received his PhD in Manufacturing Engineering from Arts et Métiers ParisTech (France) in 1999. In 2006, he received his Habilitation to Manage Research (HDR) from the University of Lyon (France). Currently, he is a Full Professor at Arts et Metiers ParisTech and manages the research laboratory named LaBoMaP since 2012. He develops his main research activities on difficult-to-cut work materials, five-axis machining, thermo mechanical modelling, development of in-situ sensor in order to understand the mechanisms of chip formation. He has followed up to now 13 PhD students and published more than 40 papers in international journals.

X. Zhu holds an Arts et Metiers engineering degree from Arts et Metiers ParisTech (France in 2012) and an MSc in Materials Engineering from Shanghai Jiao Tong University (China in 2013). She worked on materials characterisation. She is actually involved in industrial projects as a research engineer in an international company in Shanghai, China.

## 1 Introduction

With the development of cutting processes, machinists are looking for higher and higher performance of cutting tools. Proved by the worldwide researchers, the preparation of the cutting edge may bring two advantages to the commercialised cutting inserts: on one hand, the improvement consists in generating a high quality and defect-free cutting tool surface for following coating stages. On the other hand, it allows the achievement of a well-defined micro-geometry of the cutting edge. As a consequence, edge preparation affects tool life, so the economical aspect can be improved. Nevertheless, as tool wear has also an influence on the cutting mechanics during the machining operation, it affects the cutting forces.

In fact, to monitor tool wear online, dynamometers have been extensively used (Martin et al., 1986) in order to get cutting forces and torques. However, for tool wear prediction, posteriori data treatment methodologies are needed. For example, a neural network is used for nonlinear and multi-variable curve-fitting capability (Lee et al., 1998). Such technique within statistical and sensitivity analysis is based on orthogonal matrixes and the analysis of variance as proposed by Taguchi (1987). For tool wear prediction, another technique based on PCA is used for linear and multi-variable curve-fitting within a mathematical way. This technique allows the reduction of a complex correlation system into a minimal number of dimensions (Jolliffe, 2002). Indeed, Zhou et al. (2009) and Stanley et al. (2014) have demonstrated that based on relevant features extracted from forces measurements in milling, tool wear can be predicted. As previously presented, probable mechanical and geometrical changes can be revealed when the cutting edge is prepared. Indeed, when tool life is the criterion, edges with different preparations do not behave the same way. Furthermore, to identify the correlation between wear and the cutting mechanisms, it seems necessary to pick up the most suitable combination of forces for a reliable prediction of tool wear during the machining process. In light of this finding, a statistical linear model is needed to outfit the experimental and calculated evolutions.

Building on our research, the present study deals with the prediction of flank wear by cutting forces analysis, besides it highlights the influence of the cutting edge preparation method on tool wear during face milling AISI 4140 QT steel. Indeed, the cutting tests, the work material and the inserts are described in a first part. Then, the main results of the inserts profiles are shown and discussed. After that, the results of tool life tests are demonstrated by comprehensive wear charts in terms of both maximal flank wear ( $V_{Bmax}$ ) and average flank wear ( $V_{Bav}$ ) comparing the different preparation methods impacts. Moreover, to correlate cutting forces and working angles with wear results, a mechanical analysis is established using principal component analysis (PCA) leading to a statistical model for flank wear prediction.

## 2 Experimental investigation

The object of the experimental study is to compare the flank wear evolution of the untreated insert with other prepared ones, besides the evolution of the cutting forces during the trials. Through systematical analysis, the impact of edge preparation

techniques will be revealed. This study is a complementary research work to the project led by Bouzakis et al. (2014) in the frame of a CIRP collaborative working group. Consequently, the same conditions defined by the corresponding Robin test have been followed.

## 2.1 Work material

All experiments are performed with workpieces made of AISI 4140 QT (ISO 42 Cr Mo 4 QT). It is a low alloy quenched and tempered steel. Its chemical composition and mechanical properties have been determined (cf. Table 1). This alloy is widely used where there is a requirement for elevated strength in combination with a defined and high level of toughness.

**Table 1** Chemical composition and mechanical properties of AISI 4140 QT

<i>Properties</i>	<i>AISI 4140 QT</i>	
Composition in weight %	C	0.48
	Cr	1.16
	Cu	0.188
	Mn	0.882
	Mo	0.17
	Ni	0.114
HRC	31	
HB	298	
R <sub>m</sub> [MPa]	860~1,060	
R <sub>p0.2</sub> [MPa]	730	
A [%]	14	
Z [%]	45	

## 2.2 Face milling tool characteristics

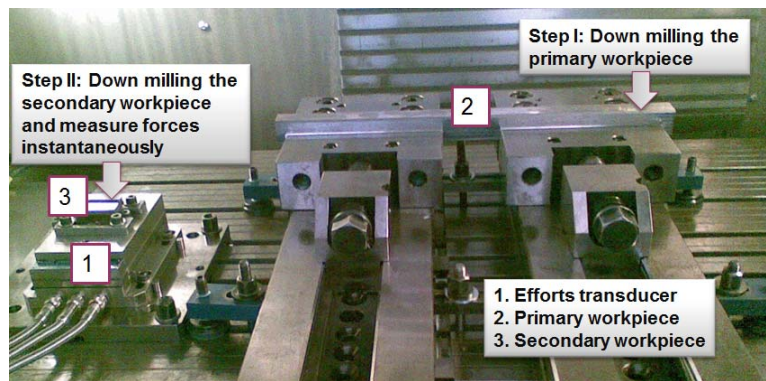
In this study, cemented carbide inserts SEAN 1203AFTN-M14 provided by SECO are used with the face milling tool SECO R220.14-0080-12 (Ø80 mm;  $\kappa_r = 45^\circ$ ). The differences among the inserts (edge radius, chamfer length) are due to the preparation process. Two types of pre-treatment are used: dragging and magneto-abrasive machining. A TiAlN coating is deposited on the inserts by physical vapour deposition (PVD) to improve the wear resistance of the grade. PVD-coated grades are recommended for applications with low feed rate where high edge toughness is required. They are suitable for applications with low to intermediate cutting speeds.

The inserts profile measurements are performed by different devices: an optical vertical scanning interferometer (VSI), a mechanical profiler and a scanning electron microscope (SEM) with stereoscopy software.

### 2.3 Milling tests

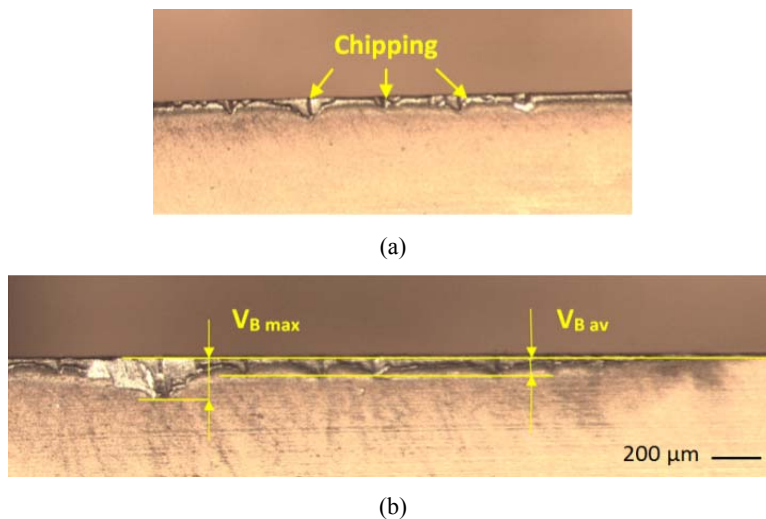
Down face milling tests are conducted on a CNC machine at a cutting speed of 250 m/min without lubrication. All experiments are carried out using only one insert at once with a 0.485 mm/tooth feed rate, a 4.7 mm and a 3 mm radial and axial engagement respectively.

**Figure 1** Experimental equipment (see online version for colours)



As Figure 1 shows the primary workpiece has a 500 mm length and a  $50 \times 50 \text{ mm}^2$  square section. The tool has to perform on 2,500 mm cutting length in order to progress the tool wear. Then, it has to cut a secondary workpiece fixed on a piezoelectric dynamometer in order to measure the cutting forces. After each forces measurement test, tool wear is inspected by an optical microscope.

**Figure 2** Worn reference edge after performing over (a) 90,000 NC corresponding to the chipping prevailing (b) 150,000 NC corresponding to the cutting edge end of life (see online version for colours)



A maximal flank wear ( $V_{Bmax}$ ) equal to 0.2 mm is chosen as tool life criterion, owing to the dramatic increase in wear rate over this value. As shown in Figure 2(b),  $V_{Bav}$  describes the average wear land of all the cutting edge area in contact with workpiece material, while  $V_{Bmax}$  describes the highest wear including the spalling depth.

## 2.4 Force measurement

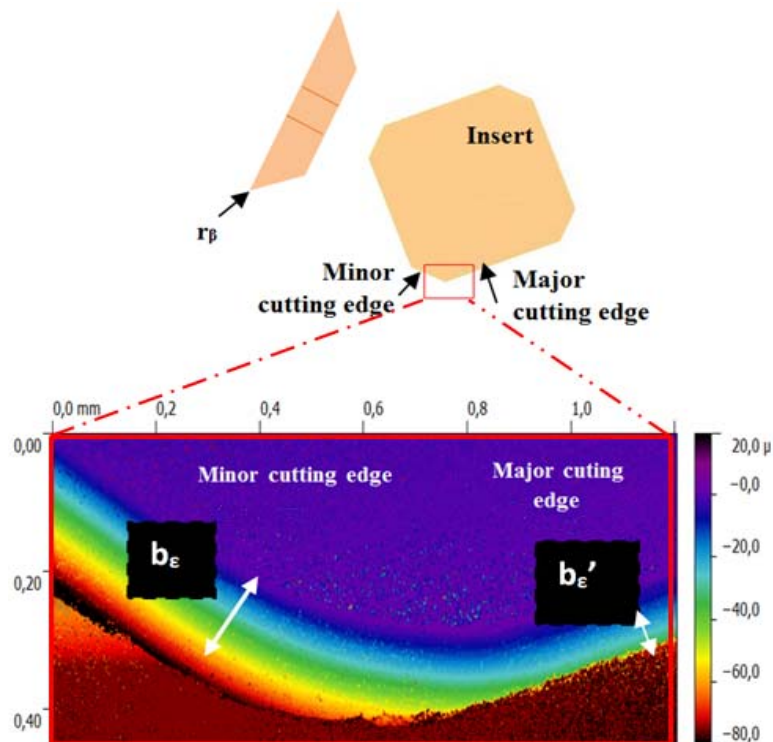
For forces monitoring, a 9257A Kistler piezoelectric dynamometer is granting the measurements, and DasyLab data acquisition software is used. For the forces  $F_x$  and  $F_y$ , the chosen measurement stretch is of  $\pm 2,000$  N, the gain of 200 N/V and the resolution is of 0.03 N. For  $F_z$ , the measurement range is of  $\pm 400$  N, the gain of 40 N/V and the resolution of 0.006 N. The sampling rate is 10 kHz.

## 3 Results and discussion

### 3.1 Influence of the edge preparations on the cutting inserts geometry

Globally, considering the minor cutting edge illustrated in Figure 3, preparations can be classified according to two criteria: the tool edge radius ( $r_\beta$ ) (from the lowest to the highest) and the chamfer length ( $b_\epsilon$ ).

**Figure 3** Chamfer corner length in major ( $b_{\epsilon'}$ ) and minor ( $b_\epsilon$ ) cutting edges characterised by optical interferometry (see online version for colours)



Those classifications lead to the same ranking. So, the untreated edge comes first, then dragging, and finally, magneto-abrasive machining as Table 2 shows.

**Table 2** Inserts cutting edges geometrical characteristics

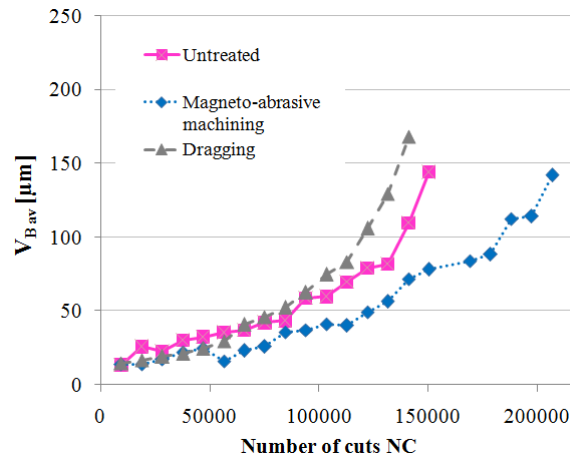
Edge preparation	Untreated		Dragging		Magneto-abrasive machining	
	Minor	Major	Minor	Major	Minor	Major
$r_\beta$ ( $\mu\text{m}$ )	37.2	37.4	42.8	44.6	53.8	52.5
$b_e$ ( $\mu\text{m}$ )	183.8	88.3	181.1	76.6	177.4	85.6

### 3.2 Wear evolution results

The milling wear test starts with a new cutting edge. Besides abrasion, small crackings appear at the beginning of the tool wear. When tool life end approaches, they are extended leaving a chipping morphology (cf. Figure 2).

Figure 4 and Figure 5 show that the insert with magneto-abrasive machining preparation has the best wear behaviour followed by the untreated insert and then dragging preparation.

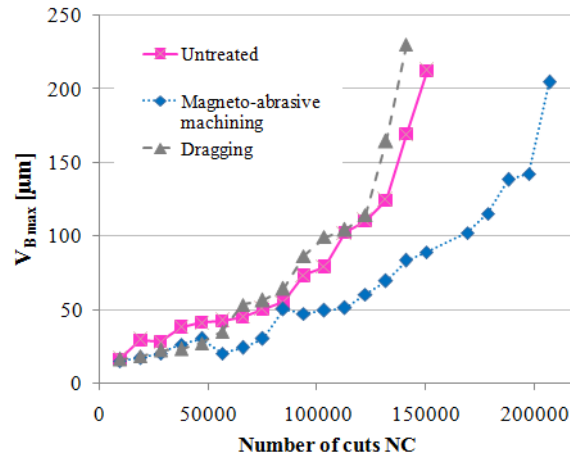
**Figure 4** Evolution of the average flank wear land ( $V_{Bav}$ ) with the different edge preparation methods (see online version for colours)



This result does not seem in agreement with the classification established according to the chamfer length or the cutting edge radius. Indeed, although the edge radius raises the edge strength against chipping, it also apparently increases flank wear (Sikdar et al., 1992); as in this particular case abrasive wear and chipping are combined, this explanation seems to be in concordance with the current results. Furthermore, other modifications may influence significantly wear resistance, such as the internal stresses of the coating and inside the substrate induced by the removal of the material, besides the influence of the surface texture on the adhesion of the coating (Rech et al., 2005).



**Figure 5** Evolution of the maximal flank wear ( $V_{Bmax}$ ) with the different edge preparation methods (see online version for colours)



### 3.3 Mechanical analysis

The second aim of this study is the definition of which parameter or combination of parameters is significantly correlated to wear evolution. So, different variables are measured during wear trials: cutting forces applied to the tool (measured directly by the piezoelectric dynamometer), and insert force components applied to the chip (calculated using data collected from the transducer and the tool geometry aspects). Those forces are essentially shear force ( $F_s$ ), normal ( $N$ ) and tangential ( $P$ ) cutting force components according to the rake face (cf. Figure 6).

As the insert has a working cutting edge angle  $\kappa_r$  equal to  $45^\circ$  and a  $20^\circ$  working back rake angle ( $\gamma_p$ ) (ISO 3002-1, 1982) some coordinate systems are then used to resolve the cutting force into directional components. According to Stephenson and Agapiou (2005), most analysis uses coordinate systems where one axis is parallel to either the cutting edge or the cutting velocity. Here, the referential related to the cutting edge is chosen because of the oblique cutting configuration.

In addition to the forces, some other variables are investigated: the apparent friction coefficient ( $\mu_e$ ) defined as the ratio between the tangential cutting force ( $P$ ) and the normal force ( $N$ ) as described in Figure 6, is also calculated. The equivalent axial angle (EAA); angle between the resultant force ( $R$ ) and the tool revolution axis, and the equivalent radial angle (ERA), which is measured between  $R$  and the cutting velocity direction are also investigated. Finally, the shear angle ( $\Phi$ ), which is the angle between the cutting force and shear plane inside the formed chip, is calculated online. In fact, for orthogonal cutting, Ruhong et al. (1983) assumed that the chip is formed by shearing along a single plane inclined at an angle  $\Phi$  with respect to the machined surface. However, in this study, the present case consists in oblique cutting. So, forces responsible of the shear ( $F_s$ ) and their inclination angle ( $\lambda$ ) relative to the resultant force ( $R$ ) are explored.

Once in the right local reference, the formula allowing the calculus of the previously described parameters is defined.

$$\vec{R} = \vec{F}_x + \vec{F}_y + \vec{F}_z \quad (1)$$

$$\vec{R} = \vec{N} + \vec{P} \quad (2)$$

$$\|\vec{N}\| = (F_x \cdot \cos \theta - F_y \cdot \sin \theta) \cdot \cos \gamma + F_z \cdot \sin \gamma \quad (3)$$

$$\vec{P} = \vec{F}_p + \vec{F}_{pn} \quad (4)$$

$$\|\vec{F}_{pn}\| = (F_x \cdot \sin \vartheta + F_y \cdot \cos \vartheta) \cdot \cos \kappa - ((F_x \cdot \cos \vartheta - F_y \cdot \sin \vartheta) \cdot \sin \gamma + F_z \cdot \cos \gamma) \cdot \sin \kappa \quad (5)$$

$$\|\vec{F}_p\| = (F_x \cdot \sin \vartheta + F_y \cdot \cos \vartheta) \cdot \sin \kappa + ((F_x \cdot \cos \vartheta - F_y \cdot \sin \vartheta) \cdot \sin \gamma + F_z \cdot \cos \gamma) \cdot \cos \kappa \quad (6)$$

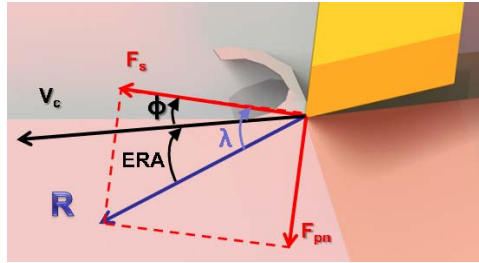
$$\|\vec{F}_c\| = F_x \cdot \cos \theta - F_y \cdot \sin \theta \quad (7)$$

$$EAA = (\vec{F}_z, \vec{R}) = \arccos(F_z / R) \quad (8)$$

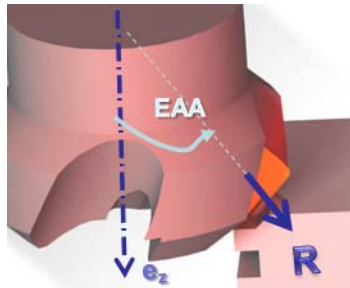
$$\beta = (\vec{N}, \vec{R}) - \arctan(P / N) \quad (9)$$

$$ERA = (\vec{R}, \vec{F}_c) = \arccos(F_c / R) \quad (10)$$

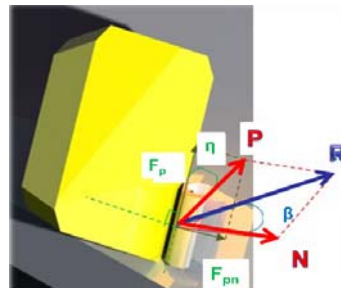
**Figure 6** Local forces and angles schema, (a) the ERA (b) the EAA (c) the apparent friction angle ( $\beta$ ) (see online version for colours)



(a)



(b)



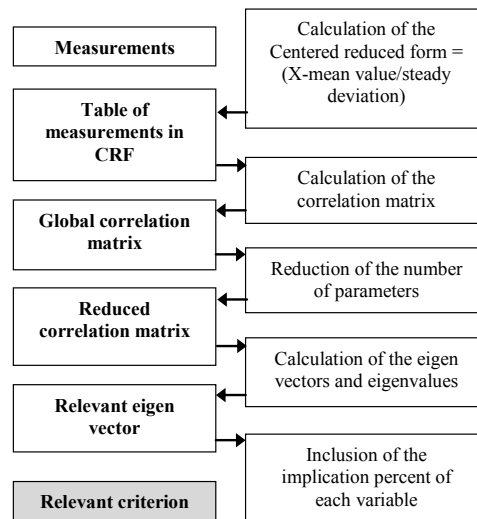
(c)

Figure 6 presents cutting force components used in the previous calculus, their position in the global and local references, and between the insert and the chip.

### 3.4 Principal component analysis

Among the different statistical methods, the PCA is the most appropriate to analyse problems including diverse measurement results. According to Jolliffe (2002), this method (PCA) is a mathematical technique that allows the reduction of a complex correlation system into a fewer number of dimensions, in order to establish the PCA criterion. Its efficiency is demonstrated by Lorenz (1989) whenever several variables are implicated in the synthesis. In this situation, measurement coding is relatively simple, since it consists in putting each variable into a centred reduced form (CRF). This form allows mathematical handling and comparison between variables which have different units and distant magnitudes. In the present study, it must be correlated with the flank wear. Figure 7 describes the sequent steps of PCA.

**Figure 7** PCA methodology



A single correlation between two variables (here  $V_B$  and one of the cutting forces components) is unable to predict tool flank wear with the required accuracy. Nonetheless, this purpose can be reached by PCA. For that reason, relying on that method, a full correlation matrix including all the components was built, and the relevant criterion (RC) was calculated. Indeed, during the tests, it was observed that the resultant force R mostly increases with the number of cuts (NC). However, its correlation with  $V_{Bmax}$  is not so obvious. Thus, R and the other mechanical parameters are analysed by PCA in order to get an elaborated relationship between the forces and flank wear.

Basing on this technique, the analysis is led. Only variables having a correlation coefficient with  $V_{Bmax}$  exceeding 62% are kept. According to this criterion, only three parameters are left to represent wear evolution:  $F_{pav}$ ,  $F_{pmav}$  and  $R_{av}$ . For the remaining parameters mentioned in Section 3.3 such as the apparent friction angle ( $\beta$ ), the corresponding correlation coefficient is below the significance threshold. Nevertheless, in

literature, for other tool-material pairs such as ceramic tool machining spheroidal cast iron, friction angle is highly correlated with the tool wear (Grzesik et al., 2014).

Then, basing on the simplified correlation matrix in Table 3(a), the factors are ranked. Indeed, eigenvalues have allowed factors classification according to their implication rate in the collected data. As factor 3 represents 89% of the significant information [the highest eigenvalue corresponding to the matrix in Table 3(a)], it is taken as the RC. According to the factor components, RC's formula is revealed as following:

$$RC = 0.596 \times F_{pav} - 0.537 \times F_{pnav} + 0.597 \times R_{av} \quad (11)$$

**Table 3(a)** Simplified correlation matrix

	$F_{pav}$	$F_{pnav}$	$R_{av}$
$F_{pav}$	1.000	-0.748	0.991
$F_{pnav}$	-0.748	1.000	-0.750
$R_{av}$	0.991	-0.750	1.000

**Table 3(b)** The different Eigen vectors

	<i>Factor 1</i>	<i>Factor 2</i>	<i>Factor 3</i>
$F_{pav}$	-0.706	0.383	0.596
$F_{pnav}$	0.004	0.844	-0.537
$R_{av}$	0.708	0.377	0.597

**Table 3(c)** Percentage of implication of every variable in Factor 3

	<i>Fact3 bis</i>
$F_{pav}$	90.9%
$F_{pnav}$	-81.8%
$R_{av}$	91.0%

**Table 3(d)** Percentage of implication of every variable in the total information

	<i>% total info</i>
$F_{pav}$	80.9%
$F_{pnav}$	-72.8%
$R_{av}$	81%

In order to quantify the real significance of the RC coefficients, they are replaced by their contribution rate in the factor 3 [corresponding to Fact3 bis cf. Table 3(c)], then multiplied by the significance rate of factor 3 (89%). So, the expression of the RC becomes:

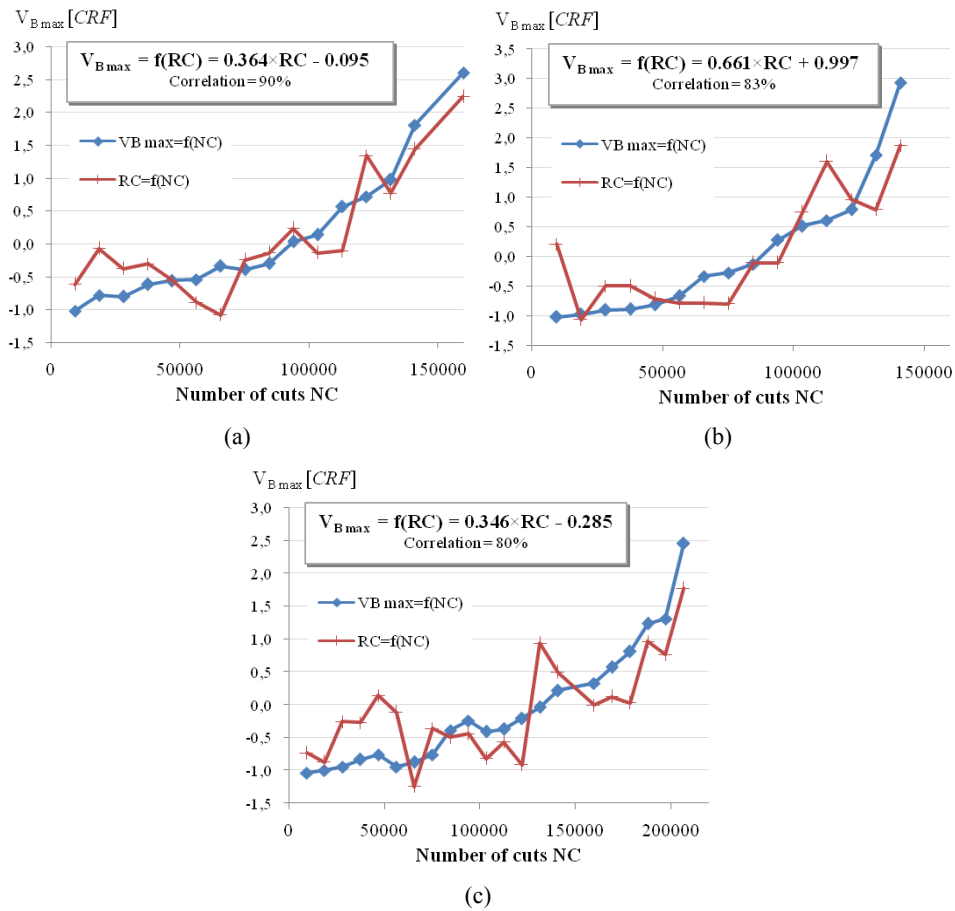
$$RC = 0.809 \times F_{pav} - 0.728 \times F_{pnav} + 0.81 \times R_{av} \quad (12)$$

In order to check if the maximal flank wear can effectively be characterised by this criterion, the correlation coefficient is calculated relating RC and  $V_{Bmax}$  for each wear test with the different edge preparation. Indeed, the referring insert flank wear is 90%, 83% and 80% correlated with the RC for the untreated edge, the one prepared by dragging and the one treated by magneto-abrasive machining respectively.

An affine relation between RC and  $V_{Bmax}$  is statistically obtained for each edge preparation (cf. Figure 8). Based on those equations,  $V_{Bmax}$  evolution graphs obtained by the RC are compared with graphs obtained by measurements. Those graphs are given in CRF calculated as following:

$$measured V_{Bmax} (CRF) = \frac{measured V_{Bmax} (\mu m) - average of V_{Bmax} (\mu m)}{steady deviation of V_{Bmax} (\mu m)} \quad (13)$$

**Figure 8**  $V_{Bmax}$  evolution obtained by measurement and by RC for (a) the untreated edge (b) the edge prepared by dragging (c) the edge prepared by magneto abrasive machining (see online version for colours)



Although the RC can only predict the CRF of the flank wear, PCA has proven its reliability. In fact, it associates parameters having different physical values (here distances in  $\mu m$  for  $V_{Bmax}$  and forces in  $N$  for cutting forces components) by transforming them into unitless variables given in CRF. Then, via the RC, the flank wear is connected to the cutting forces components. The results have shown good correlation between measurements and predictions. Indeed, Figure 8(a) shows, in the case of the untreated edge (the reference), that curves collapse with a correlation of 90%. Although the

correlation is high, the error rate is still high for edges prepared by magneto-abrasive machining (18%) and dragging (33%). Here, the best predictable behaviour is that of the reference, and the worst is the one obtained by dragging. Nevertheless, given the nature of these results, it now appears that knowing the cutting forces and the appropriate statistical model, it is possible to predict flank wear with fair approximation.

#### 4 Conclusions

This study has investigated the flank wear resistance of three inserts during AISI 4140 QT face milling and its link to cutting forces. Indeed, the statistical relationship between those cutting forces and flank wear behaviour has been demonstrated via a PCA. Furthermore, the resulting predictive laws have been built for each studied edge preparation method.

In view of the nature of the results, it has been shown that strong correlations exist between  $V_{Bmax}$  values and the machining force evolution while milling (with coefficients higher than 84%). Alongside those correlations, the mechanical and statistical analysis has revealed models predicting the flank wear. Consequently, in spite of the differences observed in the inserts behaviour, there is every likelihood that a model based on the cutting forces is able to predict online tool flank wear for each edge preparation with fair approximation. However, in light of the discussion surrounding the wear charts, it would appear likely that edge preparation does not necessarily enhance the tool wear resistance. Indeed, the untreated cutting edge has a longer tool life than the one prepared by dragging. Nevertheless, in spite of the limited number of the tested preparations, it seems possible that an optimal cutting edge radius guaranteeing the lowest tool failure exists. Therefore, it is confirmed that tool geometry is not enough to explain inserts behaviour. More research into the influence of the edge preparation on the tool surface integrity could be a good track to explain this phenomenon.

#### Acknowledgements

We gratefully thank Dr. R. M'Saoubi for providing us with the prepared inserts. We also acknowledge Pr. K.D. Bouzakis for giving us a start point to our study by making us a part of the Robin test working group investigating the effect of cutting edge preparation of coated tools on their performance in milling various materials.

#### References

- Bouzakis, K.D. et al. (2014) 'Effect of cutting edge preparation of coated tools on their performance in milling various materials', *CIRP Journal of Manufacturing Science and Technology*, Vol. 7, No. 3, pp.264–273, DOI: 10.1016/j.cirpj.2014.05.003.
- Grzesik, W., Rech, J. and Zak, K. (2014) 'Determination of friction in metal cutting with tool wear and flank face effects', *Wear*, Vol. 317, Nos. 1–2, pp.8–16, DOI: 10.1016/j.wear.2014.05.003.
- ISO 3002-1 (1982) *International Standard, Basic Quantities in Cutting and Grinding. Part 1: Geometry of the Active Part of Cutting Tools – General Terms, Reference Systems, Tool and Working Angles, Chip Breakers*, 01/08/1982.

- Jolliffe, I.T. (2002) *Principal Component Analysis*, 2nd ed., pp.1–6, Springer-Verlag, New York, DOI: 10.1002/9781118445112.stat06472.
- Lee, J.H., Kim, D.E. and Lee, S.J. (1998) ‘Statistical analysis of cutting force ratios for flank-wear monitoring’, *Journal of Materials Processing Technology*, Vol. 74, Nos. 1–3, pp.104–114, DOI: 10.1016/S0924-0136(97)00256-2.
- Lorenz, G. (1989) ‘Principal component analysis in technology’, *Annals of the CIRP*, Vol. 38, No. 1, pp.107–109, DOI: 10.1016/S0007-8506(07)62662-6
- Martin, K.F., Brandon, J.A., Grosvenor, R.I. and Owen, A. (1986) ‘A comparison of in-process tool wear measurement methods in turning’, *Proceedings of the 26th International MTDR Conference*, pp.289–295.
- Rech, J., Yen, Y-C., Schaff, M.J., Hamdi, H., Altan, T. and Bouzakis, K.D. (2005) ‘Influence of cutting edge radius on the wear resistance of PM-HSS milling inserts’, *Wear*, Vol. 259, Nos. 7–12, pp.1168–1176, DOI: 10.1016/j.wear.2005.02.072.
- Ruhong, Z., Wang, K.K. and Merchant, E. (1983) ‘Modeling of cutting force pulsation in face-milling’, *Annals of the CIRP*, Vol. 32, No. 1, pp.21–26, DOI: 10.1016/S0007-8506(07)63354-X.
- Sikdar, C., Paul, S. and Chattopadhyay, A.B. (1992) ‘Effect of variation in edge geometry on wear and life of coated carbide face milling inserts’, *Wear*, Vol. 157, No. 1, pp.111–126, DOI: 10.1016/0043-1648(92)90190-J.
- Stanley, C., Ulutan, D. and Mears, L. (2014) ‘Prediction of tool wear based on cutting forces when end milling titanium alloy Ti-6Al-4V’, *ASME 2014 International Manufacturing Science and Engineering Conference, Materials; Micro and Nano Technologies; Properties, Applications and Systems; Sustainable Manufacturing*, Detroit, Michigan, USA, 9–13 June, Vol. 1, ISBN: 978-0-7918-4580-6.
- Stephenson, D.A. and Agapiou, J.S. (2005) *Metal Cutting, Theory and Practice*, 2nd ed., pp.375–389, Taylor & Francis Group CRC Press, Boca Raton Florida, ISBN: 0824758889, 9780824758882.
- Taguchi, G. (1987) *System of Experimental Design*, Vols. 1–2, UNIPUB, Kraus, New York.
- Zhou, J.H., Pang, C.K. and Zhong Z.W. (2009) ‘Intelligent diagnosis and prognosis of tool wear using dominant feature identification’, *Industrial Informatics, IEEE*, Vol. 5, No. 4, pp.454–464, DOI: 10.1109/TII.2009.2023318.

## Nomenclature

<i>Insert geometry</i>	
$r_\beta$	Cutting edge radius
$b_e$	Chamfer corner length
$r_e$	Corner radius
References	
$(\vec{e}_x, \vec{e}_y, \vec{e}_z)$	Cartesian reference (measurements reference) linked to the workpiece
$(\vec{e}_t, \vec{e}_r, \vec{e}_z)$	Cylindrical reference (considering tool revolution axis)
$(\vec{e}_{nc}, \vec{e}_r, \vec{e}_{ic})$	Reference related to rake face
$(\vec{e}_{nc}, \vec{e}_e, \vec{e}_{fr})$	Local reference (related to cutting edge)

## Nomenclature (continued)

---

<i>Forces</i>	
$\vec{R}$	Resultant force
$\vec{F}_x$	Force measured in x direction
$\vec{F}_y$	Force measured in y direction
$\vec{F}_z$	Force measured in z direction
$\vec{N}$	Force normal to the rake face
$\vec{P}$	Force tangential to the rake face
$\vec{F}_p$	Force component parallel to the cutting edge
$\vec{F}_{np}$	Force due to friction between the chip and the face
$\vec{F}_s$	Force generating chip shear
$\vec{F}_c$	Force projection on tangential direction parallel to cutting velocity
$X_{av}$	The average value of the variable X

---

<i>Angles</i>	
$\theta_0$	Initial tool position angle
$\theta$	Tool position angle while measurement
$\kappa_r$	Tool cutting edge angle = $-45^\circ$
$\gamma$	Working rake angle = $-20^\circ$
EAA	Equivalent axial angle, between $F_z$ and R
ERA	Equivalent radial angle, between $F_c$ and R
$\beta$	Mean angle of friction between the chip and the face
$\Phi$	Shear angle (angle between $V_c$ and $F_s$ )
$\lambda$	Angle between R and $F_s$
HRC	Rockwell C hardness
HB	Brinell hardness

---

<i>Angles</i>	
$R_m$	Ultimate strength
$R_{p0.2}$	Offset yield strength
A	Elongation at break
Z	Reduction in cross section area

---

<i>Other abbreviations</i>	
CIRP	Collège International pour la Recherche en Productique
CNC	Computer numerical control
CRF	Centred reduced form
NC	Number of cuts
PCA	Principal component analysis
PVD	Physical vapour deposition
QT	Quenched and tempered
RC	Relevant criterion
SEM	Scanning electron microscope
VSI	Vertical scanning interferometry

---